Surface Plasmon–Coupled Directional Enhanced Raman Scattering by Means of the Reverse Kretschmann Configuration

ARTICLE *in* JOURNAL OF PHYSICAL CHEMISTRY LETTERS · MAY 2015

Impact Factor: 7.46 · DOI: 10.1021/acs.jpclett.5b00666

THE JOURNAL OF PHYSICAL CHEMISTRY Letters

Letter

pubs.acs.org/JPCL

Surface Plasmon-Coupled Directional Enhanced Raman Scattering by Means of the Reverse Kretschmann Configuration

Si-Xin Huo,[†] Qian Liu,[†] Shuo-Hui Cao,[†,‡] Wei-Peng Cai,[†] Ling-Yan Meng,[§] Kai-Xin Xie,[†] Yan-Yun Zhai,[†] Cheng Zong,[∥] Zhi-Lin Yang,[§] Bin Ren,[†,∥] and Yao-Qun Li*[,†]

[†]Department of Chemistry and the MOE Key Laboratory of Spectrochemical Analysis & Instrumentation, College of Chemistry and Chemical Engineering, Xiamen University, Xiamen 361005, China

[‡]Department of Electronic Science, School of Physics and Mechanical & Electrical Engineering, Xiamen University, Xiamen 361005, China

[§]Department of Physics, School of Physics and Mechanical & Electrical Engineering, Xiamen University, Xiamen 361005, China

[∥]State Key Laboratory of Physical Chemistry of Solid Surfaces, College of Chemistry and Chemical Engineering, Innovation Center of Chemistry for Energy Materials, Xiamen University, Xiamen 361005, China

Supporting Information

ABSTRACT: Surface-enhanced Raman scattering (SERS) is a unique analytical technique that provides fingerprint spectra, yet facing the obstacle of low collection efficiency. In this study, we demonstrated a simple approach to measure surface plasmon-coupled directional enhanced Raman scattering by means of the reverse Kretschmann configuration (RK-SPCR). Highly directional and p-polarized Raman scattering of 4-aminothiophenol (4-ATP) was observed on a nanoparticle-on-film substrate at 46° through the prism coupler with a sharp angle distribution (full width at half-maximum of ~3.3°). Because of the improved collection efficiency, the Raman scattering signal was enhanced 30-fold over the conventional SERS mode; this was consistent with finite-difference time-domain simulations. The effect of nanoparticles on the coupling efficiency of propagated surface plasmons was investigated. Possessing straightforward implementation and directional enhancement of Raman scattering, RK-SPCR is anticipated to simplify SERS instruments and to be broadly applicable to biochemical assays.

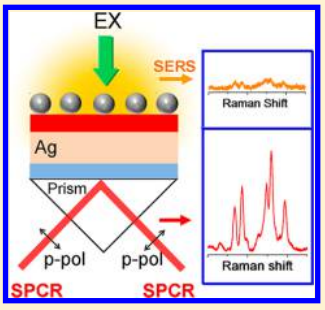

Surface plasmon-coupled emission (SPCE) is a novel near-field enhanced spectroscopy technique based on the coupling between excited molecules and propagating surface plasmons (PSPs) on a continuous metallic film. The coupling triggers the collective oscillation of surface plasmons and results in directional radiation through the prism at the surface plasmon resonance (SPR) angle for the emission wavelength.[1−3] Remarkably, SPCE is independent of the excitation mode provided that the excited molecules are located in the effective coupling region, enabling the Kretschmann (KR) and the reverse Kretschmann (RK) excitation configurations.[4,5] SPCE has been used to detect phosphorescent,[6] chemiluminescent,[7] and fluorescent species. Owing to its unique properties of highly directional emission, p-polarization, wavelength resolution, and distance dependence, SPCE has emerged as an advanced tool in fluorescence detection, with the potential for a 1000-fold improvement in the sensitivity.[1,8,9] SPCE has been applied to biochemical sensing[10−12] and fluorescence imaging;[13−15] However, although it is a general radiation coupling strategy, SPCE has been used less often in the area of Raman scattering.[16−19]

Surface-enhanced Raman scattering (SERS) is a powerful technique for direct multiplex analysis in complex systems, and it exploits the dramatically enhanced electromagnetic (EM) field of metal nanostructures to improve the Raman intensity;[20−22] however, because of the various nanostructures shapes, the EM field is inhomogeneous and suffers from a poor collection efficiency. The PSP-coupled strategy was presumed to lead to a more controllable plasmonic structure by providing a uniform enhancement of the EM field. Gratings, plasmonic antennas, and prisms have been designed to generate PSP coupling. Optimization of the gratings and plasmonic antennas can concentrate the Raman scattering at small divergence angles to achieve a high collection efficiency.[23−25] Nevertheless, the requirement for a sophisticated preparation process is an inherent limitation of the gratings and antennas. Compared with these approaches, prism coupling based on the KR configuration is a simpler approach to achieve PSP coupling and has been applied to combine SERS with SPR,[17,18,26,27] total internal reflection (TIR),[28−31] and plasmon waveguide resonance (PWR).[32,33] The effective coupling of PSPs guarantees high incident light harvesting at the SPR angle, enhancing the Raman signal. Most of these studies used light incidence from a certain angle but did not measure the directional emission. The Raman scattering captured on the air side is analogous to surface plasmon field-enhanced free-space

Received: March 31, 2015
Accepted: May 13, 2015

DOI: 10.1021/acs.jpclett.5b00666
J. Phys. Chem. Lett. 2015, 6, 2015−2019

emission (SPFS), which cannot improve the collection efficiency of the Raman signal. In KR-SPCE, Raman scattering captured on the prism side is highly directional, thereby boosting the collection efficiency of Raman scattering.[16−19,34,35] A further 20−50-fold amplification can be obtained by combining PSPs with localized surface plasmons (LSPs);[16,36] however, precise adjustment of the incident angle (full width at half-maximum (fwhm) of ∼0.5°) in the KR configuration renders it difficult in practice. Compared with the KR configuration, the RK configuration is a simple and efficient method of measuring SPCE because it is independent of the excitation angle. Hence, this RK configuration can be an impactful strategy to achieve a stronger enhancement and higher collection efficiency of Raman scattering than that obtained using traditional Raman techniques. In this study, we proposed a surface plasmon-coupled directional enhanced Raman scattering technique using the RK configuration (RK-SPCR). Using a nanoparticle-on-film substrate, the SPCR properties of 4-aminothiophenol (4-ATP), including angle distribution, polarization, and the coupling efficiency of PSPs, were investigated and compared with the results obtained from finite-difference time-domain (FDTD) simulations. By changing the nanoparticle surface coverage, we illustrated the influence of LSPs on the PSP coupling efficiency. We demonstrated that because of its high directionality and convenient implementation, RK-SPCR is an elegant approach for improving SERS collection efficiency, enhancing detection sensitivity, and simplifying the detection apparatus.

The RK configuration for recording directional Raman spectra (SPCR) on the prism side and the conventional SERS on the air side is schematically shown in Figure 1. The direction

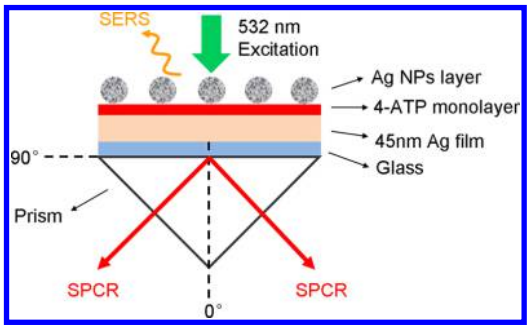

Figure 1. Reverse Kretschmann (RK) configuration for directional Raman scattering and conventional SERS observation and simulation.

normal to the sample slide interface on the prism side was defined as 0°. The RK configuration was set on the sample stage with the 532 nm laser incident from the normal direction to the sample surface. (See Figure S1 in Supporting Information.) The Raman scattering of the probe molecules (4-ATP) was collected at emission angles over the 41−51° range (Figure 2a). The Raman signal clearly exhibited angular resolution, and the strongest Raman scattering was obtained at 46°. The directional scattering was distributed at a sharp emission angle on the prism side (inset of Figure 2a). The fwhm's of the angular distributions of the different Raman bands were estimated as ∼3.3° (Figure S2 in Supporting Information), indicating that SPCR was highly directional. The emission angle became larger for smaller wavenumber in the Raman band, which agreed with the wavelength resolution in SPCE theory.[2,8,25] The angle shift was slight due to the small wavelength difference between the Raman bands. Benefit from

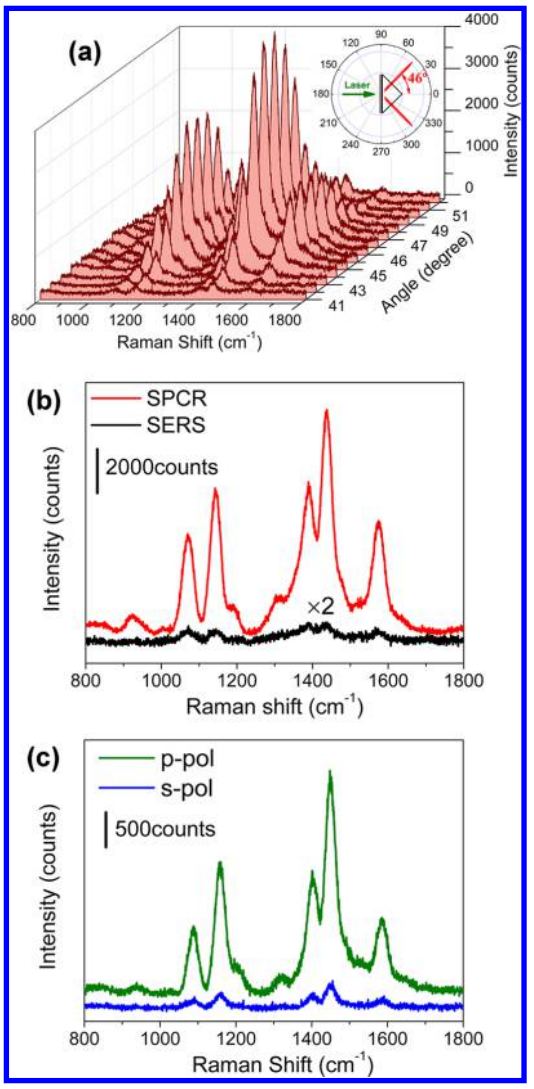

Figure 2. (a) Angle-resolved Raman spectra of 4-ATP recorded on the prism side. The inset shows the angular distribution of SPCR at 1436 cm^{-1}. (b) SPCR and SERS of 4-ATP observed from the sample. SERS intensity was multiplied by 2. (c) SPCR with p-polarization (p-pol) and s-polarization (s-pol). All spectra were recorded under 532 nm laser excitation. The laser power incident on the sample was 0.64 mW/mm^2. The Ag NP surface coverage was 6.3 NP/μm^2.

the angular and wavelength resolution of SPCR, Rayleigh, and other scattering can be readily eliminated. A simple rotation of the rotary stage from the prism side to the air side enabled this device to acquire traditional SERS spectra without any modification of the collection optics (inset of Figure S1 in Supporting Information). As shown in Figure 2b, the strong 4-ATP SPCR signal was clearly observed, while the relatively weak SERS signal was generated, by laser excitation with a power of 0.64 mW/mm^2. The major Raman spectral features were attributed to 4,4′-dimercaptoazobenzene (DMAB) because most of the 4-ATP molecules were transformed into DMAB, which is an azo dimer of 4-ATP.[37−40] The Raman intensity on the prism side was amplified by ∼30 times compared with that on the air side due to the directionality of SPCR. This demonstrates that the collection efficiency of Raman scattering was improved by the high directionality of SPCR, which is favorable for simplifying instrumentation through the reduction of the number of optical components.

DOI: 10.1021/acs.jpclett.5b00666
J. Phys. Chem. Lett. 2015, 6, 2015−2019

In SPCE, p-polarization provides the most convincing evidence of PSP coupling;[3] therefore, SPCR polarization was investigated. As shown in Figure 2c, the SPCR was found to be nearly p-polarized. It indicates that the SPCR signal through the prism originated from the interaction between the Raman dipoles and the PSPs. According to the SPCE principle, the probe molecules acting as emitting dipoles near the metallic surface can couple to PSPs and directionally radiate into the prism by matching wave vector.[19] The unusual p-polarized selectivity in RK-SPCR demonstrates that the coupling of PSPs and Raman dipoles occurred; this coupling is the origin of the high directivity.

To evaluate the collection improvement derived from the RK-SPCR directionality, we simulated directional EM field patterns on the prism and air sides using FDTD solutions software (Lumerical Solutions). According to the scanning electron microscope (SEM) images of Ag nanoparticles (NPs) on the film surface (Figure S3a–f in Supporting Information), distances between the nearest-neighbor NPs were longer than 25 nm, even for a high density of Ag NPs; therefore, no coupling should occur between the Ag NPs.[41] Thus, the simulation model was based on a single Ag NP-on-Ag film structure with a molecular dipole in the 1 nm gap between the NP and the film (Figure 1). The Ag film thickness and the Ag NP diameter were assumed as 45 and 50 nm, respectively. As shown in Figure 3a, the largest electric field enhancement occurred in the gap between the NP and the film due to the excited LSPs. Figure 3b shows the directional emission pattern at 576 nm (1436 cm^{-1}) in the far field. The maximum electric field on the prism side appears ~48° from the normal axis, in agreement with the experimental SPCR angle of 46°. Additionally, the intensity on the prism side was ~33 times stronger than that on the air side, consistent with the 30-fold enhancement observed in the RK-SPCR experiment. According to the SPCE theory,[1−3] in the RK configuration, LSPs are first excited by the incident light, inducing the excitation of 4-ATP in the NP-film gaps. Subsequently, the emitting dipoles are further coupled to PSPs supported at the interface, generating p-polarized and enhanced Raman scattering concentrated into a very narrow angle. Our experimental results demonstrate that a dramatically high collection efficiency and enhancement of Raman scattering can be achieved by exploiting RK-SPCR.

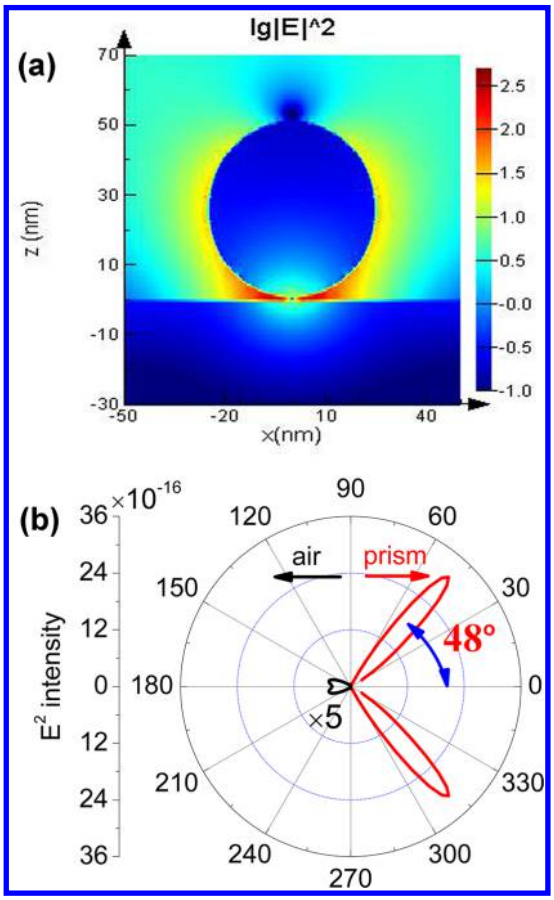

Figure 3. FDTD simulation results of (a) near field and (b) directional pattern on the prism side (red curve) and air side (black curve) at 576 nm (1436 cm^{-1}). E^2 on the air side was multiplied by 5.

To elucidate the effect of LSPs on the PSPs coupling in the RK configuration, we investigated SPCR, conventional SERS and their polarization on a series of substrates with different Ag NP surface coverages. We defined the coupling efficiency of PSPs as the intensity ratio of SPCR to conventional SERS. An increased concentration of colloidal Ag NP in the sample preparation process led to an S-shaped increased in the NP surface coverage (Figure S3g in Supporting Information). As shown in Figure 4a, the coupling efficiency increased as the NP coverage increased, reaching a peak at 6.3 NP/μm^2 and then decreasing. The ratio of the p-polarized signal to the s-polarized signal in SPCR (Figure 4b) showed a tendency similar to that of the coupling efficiency in Figure 4a. This is because p-polarization is a crucial feature of PSP coupling that can also reveal the coupling efficiency of PSP; however, the polarization ratio in SERS changed only slightly for different coverages and was markedly lower than that in SPCR, demonstrating that the PSP coupling process in SERS was weak and virtually unaffected by the coverage variation. This observation shows that the NP surface coverage influenced the PSP coupling efficiency in SPCR. On the one hand, the coupling efficiency increased while increasing coverage because a higher number of

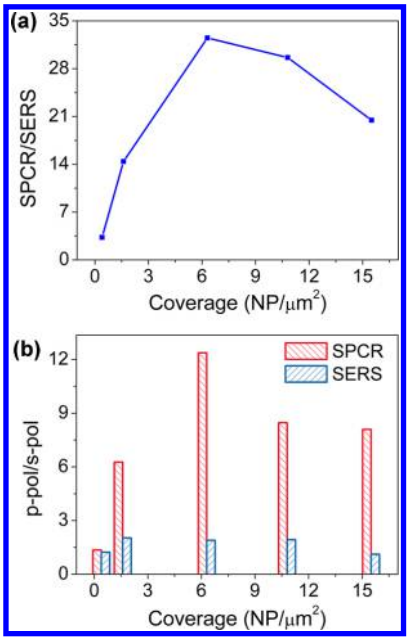

Figure 4. (a) Raman intensity ratio of SPCR to SERS at 1436 cm^{-1} and (b) ratio of the p-polarized signal to the s-polarized signal for SPCR and SERS for different Ag NP surface coverages.

DOI: 10.1021/acs.jpclett.5b00666
J. Phys. Chem. Lett. 2015, 6, 2015−2019

active "hot spots" were formed. An intense hybrid field consisting of the LSPs and PSPs was confined in the narrow gap between the NP and the metal film. PSPs were intensified by the hybrid field, providing the ultrastrong coupling of PSPs and emitting dipoles.[42,43] On the other hand, a higher Ag NP coverage on the smooth metal film causes broadening and higher reflectance in the SPR curve. The theory of coupling between LSPs on NPs and PSPs on metal film has been widely used to explain these perturbations in SPR.[43−45] Similarly, excessive LSPs couple to PSPs and perturb the coupling of PSPs and emitting dipoles in SPCR. Therefore, the coupling efficiency reduction at a higher coverage should be derived from the perturbation of the LSPs. Ag NPs simultaneously provide LSPs enhancement for PSPs and give rise to interference for the coupling of PSPs and emitting dipoles. Hence, the NP surface coverage is a critical factor for achieving optimal SPCR.

In conclusion, we proposed a simple strategy to improve the collection efficiency and sensitivity of Raman scattering. Utilizing the RK configuration, SPCR was observed to be distributed at sharp angles (fwhm of ∼3.3°) on NP-on-film structures. Compared with the conventional SERS, an approximate 30-fold enhancement was demonstrated, in agreement with the FDTD simulation. The p-polarized specificity was observed in SPCR, which can facilitate biomolecular orientation studies in complex systems. The coupling efficiency of PSPs and emitting dipoles closely related to SPCR performance can be optimized by modifying the NP density. Importantly, this RK configuration is simple to construct and achieve SPCR that avoids illumination at the SPR angle. Therefore, RK-SPCR shows great potential to develop miniaturized SERS facilities and light-emitting devices and to serve as a cost-effective tool in molecular structure and biochemical sensing studies.

EXPERIMENTAL METHODS

Ag NPs were synthesized as described by Lee et al.[46] In brief, 1 mL of 1% trisodium citrate aqueous solution was added dropwise into 50 mL of boiling 1 mM $AgNO_3$ aqueous solution under vigorous stirring. The mixture was boiled and refluxed with stirring for 1 h following and then cooled to room temperature. The size of the synthesized Ag NPs was measured as ∼50 nm by transmission electron microscope (TEM). (See Figure S4 in Supporting Information.)

For the preparation of the sample slide, a 45 nm thick Ag film was deposited on a quartz slide within 2 nm of Cr as an adhesion layer by magnetron sputtering. The fresh Ag film was immersed in 1 mM 4-ATP ethanol solution overnight to form a self-assembled monolayer. Then, a series of dilutions of colloidal Ag NP (500 μL) was dropped on the 4-ATP-modified Ag film to allow adsorption for 3 h to obtain a well-dispersive Ag NP layer. After every fabrication step, the slide was rinsed by ultra pure water and dried under nitrogen. A Hitachi S-4800 scanning electron microscope was used to image the samples and measure the Ag NP surface coverages.

Utilizing a laboratory-built multifunctional spectrometer, the Raman spectra and polarization pattern of 4-ATP excited in the RK configuration were examined (Figure S1 in Supporting Information).[10,11,42] The sample slide attached to a BK7 triangular prism via a refractive-index matching fluid was precisely positioned on the sample stage. The incident light of a 532 nm laser was normal to the sample interface with a laser spot diameter of 3 mm. By rotating the rotary stage, the SPCR on the prism side and the conventional SERS on the air side were collected through a K9 planoconvex lens (f = 120 mm) and a fiber and were then recorded by a monochromator (Andor, SR500i-D1) equipped with a CCD camera. When measuring the polarization, a polarizer was placed in the optical path used for collection. Rayleigh scattering of the analyte was blocked by a 532 nm long-pass filter. Additional details are presented in the Supporting Information.

ASSOCIATED CONTENT

Supporting Information

Details of the RK-SPCR experimental setup, angular distributions at different Raman bands, the surface coverages, and TEM image of Ag NPs. The Supporting Information is available free of charge on the ACS Publications website at DOI: 10.1021/acs.jpclett.5b00666.

AUTHOR INFORMATION

Corresponding Author

*E-mail: yaoqunli@xmu.edu.cn. Tel/Fax: (+86) 592-2185875.

Notes

The authors declare no competing financial interest.

ACKNOWLEDGMENTS

This work was supported by the 973 Program of China (2013CB933703), National Natural Science Foundation of China (21375111, 21127005, and 11474239), and the funds of the Ministry of Education of China (20110121110011 and IRT13036).

REFERENCES

(1) Lakowicz, J. R. Radiative Decay Engineering 3. Surface Plasmon-Coupled Directional Emission. *Anal. Biochem.* **2004**, *324*, 153−169.

(2) Gryczynski, I.; Malicka, J.; Gryczynski, Z.; Lakowicz, J. R. Radiative Decay Engineering 4. Experimental Studies of Surface Plasmon-Coupled Directional Emission. *Anal. Biochem.* **2004**, *324*, 170−182.

(3) Cao, S.-H.; Cai, W.-P.; Liu, Q.; Li, Y.-Q. Surface Plasmon-Coupled Emission: What Can Directional Fluorescence Bring to the Analytical Sciences? *Annu. Rev. Anal. Chem.* **2012**, *5*, 317−336.

(4) Geddes, C. D.; Gryczynski, I.; Malicka, J.; Gryczynski, Z.; Lakowicz, J. R. Directional Surface Plasmon Coupled Emission. *J. Fluoresc.* **2004**, *14*, 119−123.

(5) Gryczynski, I.; Malicka, J.; Gryczynski, Z.; Lakowicz, J. R. Surface Plasmon-Coupled Emission with Gold Films. *J. Phys. Chem. B* **2004**, *108*, 12568−12574.

(6) Previte, M. J. R.; Aslan, K.; Zhang, Y.; Geddes, C. D. Surface Plasmon Coupled Phosphorescence (SPCP). *Chem. Phys. Lett.* **2006**, *432*, 610−615.

(7) Chowdhury, M. H.; Malyn, S. N.; Aslan, K.; Lakowicz, J. R.; Geddes, C. D. First Observation of Surface Plasmon-Coupled Chemiluminescence (SPCC). *Chem. Phys. Lett.* **2007**, *435*, 114−118.

(8) Sathish, R. S.; Kostov, Y.; Rao, G. Spectral Resolution of Molecular Ensembles under Ambient Conditions Using Surface Plasmon Coupled Fluorescence Emission. *Appl. Opt.* **2009**, *48*, 5348−5353.

(9) Ray, K.; Szmacinski, H.; Enderlein, J.; Lakowicz, J. R. Distance Dependence of Surface Plasmon-Coupled Emission Observed Using Langmuir-Blodgett Films. *Appl. Phys. Lett.* **2007**, *90*, 251116/1−251116/3.

(10) Cao, S.-H.; Xie, T.-T.; Cai, W.-P.; Liu, Q.; Li, Y.-Q. Electric Field Assisted Surface Plasmon-Coupled Directional Emission: An Active Strategy on Enhancing Sensitivity for DNA Sensing and Efficient Discrimination of Single Base Mutation. *J. Am. Chem. Soc.* **2011**, *133*, 1787−1789.

DOI: 10.1021/acs.jpclett.5b00666
J. Phys. Chem. Lett. 2015, 6, 2015−2019

(11) Liu, X.-Q.; Liu, Q.; Cao, S.-H.; Cai, W.-P.; Weng, Y.-H.; Xie, K.-X.; Li, Y.-Q. Directional Surface Plasmon-Coupled Emission of CdTe Quantum Dots and Its Application in Hg(ii) Sensing. *Anal. Methods* **2012**, *4*, 3956−3960.
(12) Matveeva, E.; Gryczynski, Z.; Gryczynski, I.; Malicka, J.; Lakowicz, J. R. Myoglobin Immunoassay Utilizing Directional Surface Plasmon-Coupled Emission. *Anal. Chem.* **2004**, *76*, 6287−6292.
(13) Borejdo, J.; Gryczynski, Z.; Calander, N.; Muthu, P.; Gryczynski, I. Application of Surface Plasmon Coupled Emission to Study of Muscle. *Biophys. J.* **2006**, *91*, 2626−2635.
(14) Zhang, D. G.; Moh, K. J.; Yuan, X. C. Surface Plasmon-Coupled Emission from Shaped PMMA Films Doped with Fluorescence Molecules. *Opt. Express* **2010**, *18*, 12185−12190.
(15) Cai, W.-P.; Liu, Q.; Cao, S.-H.; Weng, Y.-H.; Liu, X.-Q.; Li, Y.-Q. Prism-Based Surface Plasmon Coupled Emission Imaging. *ChemPhysChem* **2012**, *13*, 3848−3851.
(16) Du, L.; Tang, D.; Yuan, G.; Wei, S.; Yuan, X. Emission Pattern of Surface-Enhanced Raman Scattering from Single Nanoparticle-Film Junction. *Appl. Phys. Lett.* **2013**, *102*, 081117.
(17) Meyer, S. A.; Le Ru, E. C.; Etchegoin, P. G. Combining Surface Plasmon Resonance (SPR) Spectroscopy with Surface-Enhanced Raman Scattering (SERS). *Anal. Chem.* **2011**, *83*, 2337−2344.
(18) Meyer, S. A.; Auguié, B.; Le Ru, E. C.; Etchegoin, P. G. Combined SPR and SERS Microscopy in the Kretschmann Configuration. *J. Phys. Chem. A* **2012**, *116*, 1000−1007.
(19) Li, H.; Xu, S.; Liu, Y.; Gu, Y.; Xu, W. Directional Emission of Surface-Enhanced Raman Scattering Based on a Planar-Film Plasmonic Antenna. *Thin Solid Films* **2012**, *520*, 6001−6006.
(20) Haynes, C. L.; McFarland, A. D.; Duyne, R. P. V. Surface-Enhanced Raman Spectroscopy. *Anal. Chem.* **2005**, *77*, 338 A−346 A.
(21) Li, J. M.; Wei, C.; Ma, W. F.; An, Q.; Guo, J.; Hu, J.; Wang, C. C. Multiplexed SERS Detection of DNA Targets in a Sandwich-Hybridization Assay Using SERS-Encoded Core-Shell Nanospheres. *J. Mater. Chem.* **2012**, *22*, 12100−12106.
(22) Boca-Farcau, S.; Potara, M.; Simon, T.; Juhem, A.; Baldeck, P.; Astilean, S. Folic Acid-Conjugated, SERS-Labeled Silver Nanotriangles for Multimodal Detection and Targeted Photothermal Treatment on Human Ovarian Cancer Cells. *Mol. Pharmaceutics* **2013**, *11*, 391−399.
(23) Kahl, M.; Voges, E. Analysis of Plasmon Resonance and Surface-Enhanced Raman Scattering on Periodic Silver Structures. *Phys. Rev. B: Condens. Matter Mater. Phys.* **2000**, *61*, 14078−14088.
(24) Wang, D.; Yang, T.; Crozier, K. B. Optical Antennas Integrated with Concentric Ring Gratings: Electric Field Enhancement and Directional Radiation. *Opt. Express* **2011**, *19*, 2148−57.
(25) Gu, Y.; Li, H.; Xu, S.; Liu, Y.; Xu, W. Evanescent Field Excited Plasmonic Nano-Antenna for Improving SERS Signal. *Phys. Chem. Chem. Phys.* **2013**, *15*, 15494−15498.
(26) Liu, Y.; Xu, S.; Tang, B.; Wang, Y.; Zhou, J.; Zheng, X.; Zhao, B.; Xu, W. Note: Simultaneous Measurement of Surface Plasmon Resonance and Surface-Enhanced Raman Scattering. *Rev. Sci. Instrum.* **2010**, *81*, 036105/1−036105/3.
(27) Liu, Y.; Xu, S.; Xuyang, X.; Zhao, B.; Xu, W. Long-Range Surface Plasmon Field-Enhanced Raman Scattering Spectroscopy Based on Evanescent Field Excitation. *J. Phys. Chem. Lett.* **2011**, *2*, 2218−2222.
(28) Futamata, M. Surface-Plasmon-Polariton-Enhanced Raman Scattering from Self-Assembled Monolayers of p-Nitrothiophenol and p-Aminothiophenol on Silver. *J. Phys. Chem.* **1995**, *99*, 11901−11908.
(29) Du, L.; Yuan, G.; Tang, D.; Yuan, X. Tightly Focused Radially Polarized Beam for Propagating Surface Plasmon-Assisted Gap-Mode Raman Spectroscopy. *Plasmonics* **2011**, *6*, 651−657.
(30) McKee, K. J.; Meyer, M. W.; Smith, E. A. Near IR Scanning Angle Total Internal Reflection Raman Spectroscopy at Smooth Gold Films. *Anal. Chem.* **2012**, *84*, 4300−4306.
(31) Yih, J.-N.; Chen, S.-J.; Huang, K.-T.; Su, Y. T.; Lin, G. Y. A Compact Surface Plasmon Resonance and Surface-Enhanced Raman Scattering Sensing Device. *Proc. SPIE* **2004**, *5327*, 5−9.
(32) McKee, K. J.; Meyer, M. W.; Smith, E. A. Plasmon Waveguide Resonance Raman Spectroscopy. *Anal. Chem.* **2012**, *84*, 9049−9055.
(33) Gu, Y.; Xu, S.; Li, H.; Wang, S.; Cong, M.; Lombardi, J. R.; Xu, W. Waveguide-Enhanced Surface Plasmons for Ultrasensitive SERS Detection. *J. Phys. Chem. Lett.* **2013**, *4*, 3153−3157.
(34) Corn, R. M.; Philpott, M. R. Surface Plasmon-Enhanced Raman Scattering at Thin Silver Films. *J. Chem. Phys.* **1984**, *80*, 5245−5249.
(35) Giergiel, J.; Reed, C. E.; Hemminger, J. C.; Ushioda, S. Surface Plasmon Polariton Enhancement of Raman Scattering in a Kretschmann Geometry. *J. Phys. Chem.* **1988**, *92*, 5357−5365.
(36) Liu, Y.; Xu, S.; Li, H.; Jian, X.; Xu, W. Localized and Propagating Surface Plasmon Co-enhanced Raman Spectroscopy Based on Evanescent Field Excitation. *Chem. Commun.* **2011**, *47*, 3784−3786.
(37) Fang, Y.; Li, Y.; Xu, H.; Sun, M. Ascertaining p,p′-Dimercaptoazobenzene Produced from p-Aminothiophenol by Selective Catalytic Coupling Reaction on Silver Nanoparticles. *Langmuir* **2010**, *26*, 7737−7746.
(38) Huang, Y.-F.; Zhu, H.-P.; Liu, G.-K.; Wu, D.-Y.; Ren, B.; Tian, Z.-Q. When the Signal Is Not from the Original Molecule To Be Detected: Chemical Transformation of para-Aminothiophenol on Ag during the SERS Measurement. *J. Am. Chem. Soc.* **2010**, *132*, 9244−9246.
(39) Huang, Y. F.; Wu, D. Y.; Zhu, H. P.; Zhao, L. B.; Liu, G. K.; Ren, B.; Tian, Z. Q. Surface-Enhanced Raman Spectroscopic Study of p-Aminothiophenol. *Phys. Chem. Chem. Phys.* **2012**, *14*, 8485−8497.
(40) Chiba, H.; Suzuki, H.; Futamata, M. Highly Sensitive Raman Spectroscopy Using a Gap Mode Plasmon under an Attenuated Total Reflection geometry. *Vib. Spectrosc.* **2014**, *73*, 19−23.
(41) Shanthil, M.; Thomas, R.; Swathi, R. S.; George Thomas, K. Ag@SiO2 Core−Shell Nanostructures: Distance-Dependent Plasmon Coupling and SERS Investigation. *J. Phys. Chem. Lett.* **2012**, *3*, 1459−1464.
(42) Cao, S.-H.; Cai, W.-P.; Liu, Q.; Xie, K.-X.; Weng, Y.-H.; Huo, S.-X.; Tian, Z.-Q.; Li, Y.-Q. Label-Free Aptasensor Based on Ultrathin-Linker-Mediated Hot-Spot Assembly to Induce Strong Directional Fluorescence. *J. Am. Chem. Soc.* **2014**, *136*, 6802−6805.
(43) Chowdhury, M. H.; Ray, K.; Geddes, C. D.; Lakowicz, J. R. Use of Silver Nanoparticles to Enhance Surface Plasmon-Coupled Emission (SPCE). *Chem. Phys. Lett.* **2008**, *452*, 162−167.
(44) Lyon, L. A.; Peña, D. J.; Natan, M. J. Surface Plasmon Resonance of Au Colloid-Modified Au Films: Particle Size Dependence. *J. Phys. Chem. B* **1999**, *103*, 5826−5831.
(45) He, L.; Smith, E. A.; Natan, M. J.; Keating, C. D. The Distance-Dependence of Colloidal Au-Amplified Surface Plasmon Resonance. *J. Phys. Chem. B* **2004**, *108*, 10973−10980.
(46) Lee, P. C.; Meisel, D. Adsorption and Surface-Enhanced Raman of Dyes on Silver and Gold Sols. *J. Phys. Chem.* **1982**, *86*, 3391−3395.

DOI: 10.1021/acs.jpclett.5b00666
J. Phys. Chem. Lett. 2015, 6, 2015−2019